JBUON 2016; 21(6): 1501-1509
ISSN: 1107-0625, online ISSN: 2241-6293 • www.jbuon.com
E-mail: editorial_office@jbuon.com

ORIGINAL ARTICLE

Identification of differential pathways in papillary thyroid carcinoma utilizing pathway co-expression analysis

Wei-Hai Qiu[1], Gui-Yan Chen[1], Lu Cui[1], Ting-Ming Zhang[1], Feng Wei[1], Yong Yang[2]

[1]Department of Endocrinology, Binzhou People's Hospital, Binzhou, 256600, Shandong Province, China; [2]Department of Breast and Thyroid Surgery, Wuhan No.1 Hospital, Wuhan, 430022, Hubei Province, China

Summary

Purpose: *To identify differential pathways between papillary thyroid carcinoma (PTC) patients and normal controls utilizing a novel method which combined pathway with co-expression network.*

Methods*: The proposed method included three steps. In the first step, we conducted pretreatments for background pathways and gained representative pathways in PTC. Subsequently, a co-expression network for representative pathways was constructed using empirical Bayes (EB) approach to assign a weight value for each pathway. Finally, random model was extracted to set the thresholds of identifying differential pathways.*

Results: *We obtained 1267 representative pathways and their weight values based on the co-expressed pathway network, and then by meeting the criterion (Weight > 0.0296), 87 differential pathways in total across PTC patients and normal controls were identified. The top three ranked differential pathways were CREB phosphorylation, attachment of GPI anchor to urokinase plasminogen activator receptor (uPAR) and loss of function of SMAD2/3 in cancer.*

Conclusions: *In conclusion, we successfully identified differential pathways (such as CREB phosphorylation, attachment of GPI anchor to uPAR and post-translational modification: synthesis of GPI-anchored proteins) for PTC using the proposed pathway co-expression method, and these pathways might be potential biomarkers for target therapy and detection of PTC.*

Key words: *differential pathway, empirical Bayes co-expression, genes, papillary thyroid carcinoma*

Introduction

PTC is the most common thyroid malignancy [1] Current treatments involve surgery, radioactive iodine treatment, and thyroid hormone suppression [2], and its current 5-year survival are >95% although the incidence is increasing, which indicates that the overall prognosis is impressively favorable [3]. However, a number of PTC patients are not readily identified by histopathologic staging and may have aggressive disease characterized by local recurrence and/or distant metastasis [4]. Therefore, early detection and diagnosis of PTC is undoubtely needed.

Currently, several molecular markers have been identified as biological indicators for PTC. For instance, a high frequency of activating somatic alterations of genes encoding effectors in the mitogen-activated protein kinase (*MAPK*) signaling pathway of PTC were identified [5], which included point mutations of B-Raf proto-oncogene and serine threonine kinase (*BRAF*) [6,7]. Mutations in members of the phosphoinositide 3-kinase (*PI3K*) pathway, such as phosphatase and tensin homolog (*PTEN*), phosphatidylinositol-4,5-bisphosphate 3- kinase, catalytic subunit alpha (*PIK3CA*), and v-akt murine thymoma viral oncogene homolog 1 (*AKT1*), have also been

Correspondence to: Yong Yang, MD. Department of Breast and Thyroid Surgery, Wuhan No.1 Hospital, No.215 on Zhongshan Avenue, Qiaokou District, Wuhan, 430022, Hubei Province, China. Tel:+86 027 85332811, Fax: +86 027 85332018, E-mail: yongyang2016@yeah.net
Received: 01/03/2014; Accepted: 21/03/2014

reported at low frequencies in PTC [8]. However, the number of these biomarkers is few and there exists a severe need for understanding PTC mechanism and customized anticancer therapies, the identification of differential pathways may help to solve this challenge to some extent.

Pathway analysis has become the first choice for gaining insight into the underlying biology of genes and proteins, as it reduces complexity and increases the explanatory power [9]. Existing pathway analysis techniques are mainly focused on only one of static or dynamic method. For example, the Database for Annotation, Visualization and Integrated Discovery (DAVID) [10] and neaGUI package [11] are static, such as a given Reactome pathway database, which may not reflect the specific conditioned pathway under study. Hence more and more researchers focused on pathways based on dynamic networks which consider network variations but produce many false-positive results resulting from various effects on the expression of their interacting genes [12]. Meanwhile, identifying pathway changes or differential pathways, will create an informative description of the biology that is occurring in a particular dataset, making it possible to generate new hypotheses and to identify genetic signatures that provide insight into understanding, diagnosing and treating disease [13,14]. Therefore, we proposed a novel method by combining static and dynamic methods together to identify differential pathways between PTC and normal controls.

The objective of this article was to propose a novel method of combined pathway identification with co-expression network, and then apply the method to detect differential pathways in PTC. To achieve this goal, firstly, representative pathways for PTC were obtained based on the background pathways. Subsequently, we constructed a co-expression network for representative pathways using EB approach to assign a weight value for each pathway. Finally, a random model was extracted to set the thresholds of identifying differential pathways. To validate the feasibility of the proposed method, we compared it with DAVID pathways enrichment analysis based on differentially expressed genes (DEGs). The differential pathways might be potential biomarkers of target therapy and might give an insight to future study of PTC.

Methods

Gene data recruitment

Two gene expression profiles of PTC (E-GEOD-33630 and E-GEOD-60542) were recruited from the online public free ArrayExpress database. E-GEOD-33630 comprised 49 PTC samples and 45 normal controls and presented on A-AFFY-44- Affymetrix GeneChip Human Genome U133 Plus 2.0 [HG-U133_Plus_2] Platform, while for E-GEOD-60542 there were a total of 63 samples (33 PTC samples and 30 normal controls), and the platform of this profile was the same as E-GEOD-33630. Therefore, in this study 82 PTC samples and 75 normal controls, and in total 167 samples were involved in the two datasets.

Data preprocessing

To control the qualities of datasets on probe-level, standard pre-treatments were performed for them. Firstly, background correction was carried out by Robust Multi-array Average (RMA) algorithm to eliminate the influence of nonspecific hybridization [15]; subsequently, normalization was conducted according to quantiles-based algorithm to make the distribution of probe intensities for each array in a set of arrays the same [16]; next, we applied Micro Array Suite (MAS) algorithm to revise perfect match and mismatch value [17]; finally, medianpolish method was selected to summarize expression values [15]. Expression structures were converted from the preprocessed data in AffyBatch formats, screened by feature filter method to discard duplicated genes based on genefilter package [18], and mapped each probe ID to gene symbol through annotate package [19]. A total of 20389 genes were obtained for E-GEOD-33630 and E-GEOD-60542, respectively.

Data merging

To remove the batch effects caused by the use of different experimentation plans and methodologies, we employed GENENORM method in inSilicoMerging package [20] to merge the two preprocessed gene expression profiles into a single group. In this method, for each gene expression value x_{ij} in each study separately, all values were modified by subtracting the mean $\bar{x}_i$ of the gene in that dataset divided by its standard deviation σ_i. Measured gene expression values ($\hat{x}_{ij}^k$) of gene i in sample j of the batch k could be expressed as:

$$\hat{x}_{ij}^k = \frac{x_{ij}^k - \bar{x}_j^k}{\sigma_i^k}$$

The merged dataset included 20389 genes and was used for further exploitation.

Pathway data

Biological pathways for human beings were downloaded from the Reactome pathway database (http://www.reactome.org), and we gained 1675 pathways in total. To make pathways more confident and stable, we discarded pathways with gene number ≤ 2, and a total

of 1639 pathways were obtained which were denoted as background pathways in the subsequent study. Reactome is a manually curated open resource for human pathway data described in molecular terms and provides infrastructure for computation across the biologic reaction network [21].

Differential pathways identification

In this paper, to identify differential pathways between PTC patients and normal controls, we proposed a method, which combined random model to screen differential pathways in conjunction with pathway co-expressed network to assign a weight for each representative pathway.

Pathway co-expression network

Before constructing pathway co-expression network, we should excavate genes enriched in pathways. To achieve this, firstly, we calculated mean gene number (*M*) for 1639 background pathways; *M* = total gene number for pathways (73099)/pathway number (1639)=44.6 and here we took *M*=44 for convenience. Secondly, for each pathway, its gene amount was denoted by *A*, and the number of its intersection with gene expression data was denoted by *B*. We selected these that satisfied with $B > 5$ and $B/A > 0.8$ as the representative pathways, and 1267 representative pathways were gained. Thirdly, EB approach [22] was implemented to conduct co-expressed network for genes of each representative pathway, and the number of possible constructed gene-gene interactions in one representative pathway was represented by *C* which equaled to

$$C = \frac{A * (A - 1)}{2}$$

In EB method, expression values of pathway genes were displayed as an *m*-by-*n* matrix, where *m* was the number of genes under any representative pathway and *n* was the total number of representative pathways. Subsequently, these values were normalized and obtained matrix *X*, of which the members took values in 1-*K*, where *K* was the total number of conditions. Based on *X*, we calculated intra-group correlations for all gene pairs, hence the resulting *Y* matrix of correlations was *l*-by-*K*. Mclust algorithm was employed to initialize the hyper parameters to find the component normal mixture model that best fitted the correlations of *Y* after transformation. Finally, those who met a soft threshold of false discovery rate (FDR) ≤ 0.05 were selected to construct the pathway co-expression network. The amount of interactions in one pathway network was marked as *D*, and *D*/*C* was defined as the weight for this pathway.

Differential pathways

To identify the differential pathways between PTC patients and normal controls based on representative pathways, a random model which consisted of *M* genes was constructed. *M* genes were randomly extracted from the gene expression data, and then EB co-expression analysis was performed to determine weight. Capturing 10000 times at random, 10000 weights were obtained, and we ranked them in descending order, and set the weight of the 100th pathway (Weight=0.0296) to be the thresholding (FDR<0.01), while representative pathways with weight >0.0296 were considered to be differential pathways.

DEGs detection

To identify DEGs between PTC and normal controls based on gene expression profiles, Linear Models for Microarray Data (LIMMA) package in R was applied [24]. Genes which met the thresholds of p <0.01 and $|\log_2 \text{FoldChange}| > 3$ were identified as DEGs.

Reactome pathway enrichment analysis

Reactome pathway enrichment analysis for DEGs was performed using the online tool DAVID which provided exploratory visualization tools that promoted discovery through functional classification, biochemical pathway maps, and conserved protein domain architectures [25]. Expression analysis systematic explored (EASE) test implemented in DAVID was used to calculate p value of each pathway. EASE is an easy-to-use, customizable tool that allows investigators to systematically mine the mass of functional information associated with data generated by microarray [26]. If one pathway was under the threshold (EASE=0.05, count >2), we considered it to be differential pathway in PTC.

Statistics

The statistical methods used in this study were: EB approach, FDR test and EASE test, each being described in relative places in Methods.

Results

Differential pathways

There were 20389 genes in the integrated gene expression data which were used for the subsequent study. Meanwhile, 1267 representative pathways were obtained based on Reactome pathway database and effective pretreatment. For each representative pathway, we assigned a weight value according to pathway EB co-expression network, and the weight distribution is illustrated in Figure 1. We found that the majority of the number of representative pathways was distributed in the section with weight ranging from 0 to 0.05, especially 0~0.01. The larger the weight of one representative pathway, the more significant the pathway in PTC was. In addition, we noticed

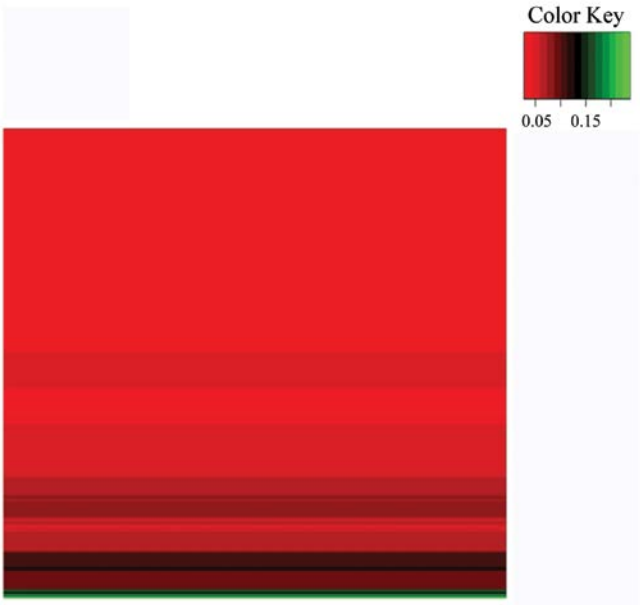

Figure 1. The heatmap for differential pathways and their weight values.

representative pathways with weight >0.0296 as differential pathways. Furthermore, a heatmap between the correlation of differential pathways and their weight values was created (Figure 1).

The 87 differential pathways are displayed in Table 1. The top 5 ranked differential pathways were CREB phosphorylation (Weight = 0.2381), attachment of GPI anchor to uPAR (Weight=0.1905), loss of function of SMAD2/3 in cancer (Weight=0.1429), SMAD2/3 MH2 domain mutants in cancer (Weight=0.1429), and interleukin-6 signaling (Weight=0.1273). The essence of one pathway was a sub-network built by enriched genes and their interactions. Hence, in this work, we constructed a network for each pathway utilizing EB approach. Because the gene number of differential pathways was different and too small number of genes might not connect to each other in whole, we selected two differential pathways with larger gene amount, post-translational modification: synthesis of GPI-anchored proteins (Count=26) and regulation of HSF1-mediated heat shock response (Count=75), and their co-expression network is shown in Figures 2 and 3, respectively. For post-translational modification: synthesis of GPI-anchored proteins pathway network, there were 21 genes and 34 edges, while 50 genes were mapped to the regulation of HSF1-mediated heat shock response network and formed 108 interactions.

Comparison with DAVID

To clarify whether differential pathways across PTC patients and normal controls was feasible or not, we compared the proposed method with traditional DAVID software. A total of 429 DEGs were explored based on Limma package with thresholds of $p < 0.01$ and $|\log_2 FoldChange| > 3$. Then, Reactome pathway enrichment analysis showed that only 12 differential pathways were determined under the condition of EASE = 0.05 and count > 2 (Table 2). The top 5 significant pathways were integrin cell surface interactions (p=0.0041), hemostasis (p=0.0043), axon guidance (p=0.0136), signaling by PDGF (p=0.0329) and hormone biosynthesis (p=0.0761).

Unfortunately, when comparing differential pathways obtained from pathway co-expression method and DAVID, no intersection was noticed. However, the quantity was far more than DAVID and differential pathways identified based on the pathway co-expression method were closely correlated to PTC.

Discussion

In this paper, we proposed a novel method by connecting pathways to EB co-expression network to identify differential pathways between PTC patients and normal controls. The results showed that a total of 87 differential pathways were identified across PTC and normal controls, such as CREB phosphorylation, attachment of GPI anchor to uPAR and post-translational modification: synthesis of GPI-anchored proteins.

CREB, cyclic AMP responsive element bind-

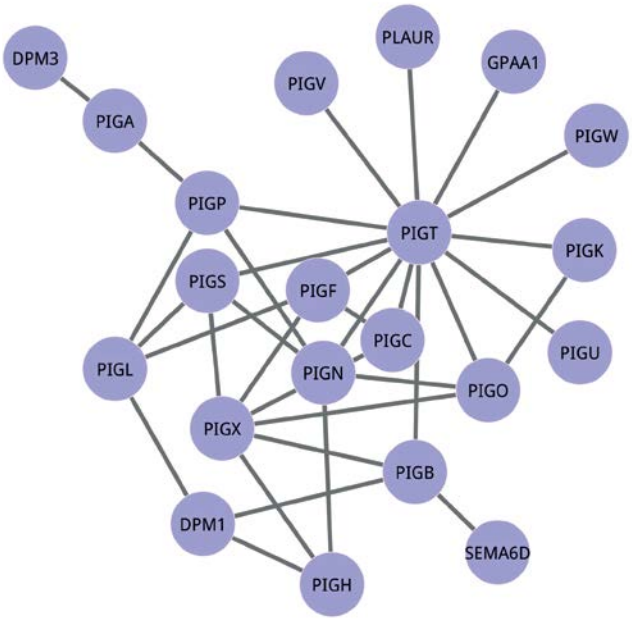

Figure 2. Co-expression network of genes in differential pathway (post-translational modification: synthesis of GPI-anchored proteins). Nodes are pathway genes, and edges stay for the interactions among genes.

Table 1. Differential pathways in PTC based on co-expression analysis

Pathway	*Weight*	*Count*
CREB phosphorylation	0.2381	7
Attachment of GPI anchor to uPAR	0.1905	7
Loss of Function of SMAD2/3 in Cancer	0.1429	7
SMAD2/3 MH2 Domain Mutants in Cancer	0.1429	7
Interleukin-6 signaling	0.1273	11
activated TAK1 mediates p38 MAPK activation	0.1250	16
Signaling by TGF-beta Receptor Complex in Cancer	0.1071	8
Sema4D mediated inhibition of cell attachment and migration	0.1071	8
Post-translational modification: synthesis of GPI-anchored proteins	0.1046	26
Activation of BAD and translocation to mitochondria	0.0953	15
CLEC7A (Dectin-1) induces NFAT activation	0.0909	11
JNK phosphorylation and activation mediated by activated human TAK1	0.0833	16
Synthesis secretion and inactivation of Glucose-dependent Insulinotropic Polypeptide	0.0758	12
HSF1 activation	0.0684	17
Regulation of HSF1-mediated heat shock response	0.0674	75
SMAD2/3 Phosphorylation Motif Mutants in Cancer	0.0667	6
Synthesis of 15-eicosatetraenoic acid derivatives	0.0667	6
TAK1 activates NFkB by phosphorylation and activation of IKKs complex	0.0633	25
Sema4D in semaphorin signaling	0.0627	27
Detoxification of Reactive Oxygen Species	0.0627	27
Synthesis secretion and inactivation of Glucagon-like Peptide-1 (GLP-1)	0.0584	19
Cellular response to heat stress	0.0571	91
Antiviral mechanism by IFN-stimulated genes	0.0570	67
ISG15 antiviral mechanism	0.0570	67
MAPK targets/ Nuclear events mediated by MAP kinases	0.055172	30
Synthesis of IP2 IP and Ins in the cytosol	0.0545	11
Intraflagellar transport	0.0526	40
Incretin synthesis secretion and inactivation	0.0519	22
Activation of BH3-only proteins	0.0507	24
Sema4D induced cell migration and growth-cone collapse	0.0507	24
TGF-beta receptor signaling in EMT (epithelial to mesenchymal transition)	0.0500	16
Loss of Function of TGFBR1 in Cancer	0.0477	7
TGFBR1 KD Mutants in Cancer	0.0477	7
Anchoring fibril formation	0.0477	7
Erythrocytes take up carbon dioxide and release oxygen	0.0477	7
Erythrocytes take up oxygen and release carbon dioxide	0.0477	7
O2/CO2 exchange in erythrocytes	0.0477	7
RHO GTPases activate CIT	0.0477	15
Signaling by FGFR1 fusion mutants	0.0458	18
Chk1/Chk2(Cds1) mediated inactivation of Cyclin B:Cdk1 complex	0.0455	12
TGF-beta receptor signaling activates SMADs	0.0452	31
Unfolded Protein Response (UPR)	0.0447	81
Signaling by TGF-beta Receptor Complex	0.0447	71
Ethanol oxidation	0.0444	10
Growth hormone receptor signaling	0.0435	24
RHO GTPases activate PAKs	0.0429	21
MAP kinase activation in TLR cascade	0.0424	55
ABC-family proteins mediated transport	0.0418	42
ZBP1(DAI) mediated induction of type I IFNs	0.0400	25
Nuclear Events (kinase and transcription factor activation)	0.0399	24
Striated Muscle Contraction	0.0387	31
Interferon alpha/beta signaling	0.0383	66
MyD88 cascade initiated on plasma membrane	0.0370	82
Toll Like Receptor 10 (TLR10) Cascade	0.0370	82
Toll Like Receptor 5 (TLR5) Cascade	0.0370	82
Transcriptional activation of mitochondrial biogenesis	0.0370	38

Continued on the next page

Translocation of GLUT4 to the plasma membrane	0.0368	59
Effects of PIP2 hydrolysis	0.0367	25
TRAF6 Mediated Induction of proinflammatory cytokines	0.0365	73
Keratan sulfate degradation	0.0364	11
Cytosolic sensors of pathogen-associated DNA	0.0362	64
TRAF6 mediated induction of NFkB and MAP kinases upon TLR7/8 or 9 activation	0.0361	83
MyD88 dependent cascade initiated on endosome	0.0350	85
Toll Like Receptor 7/8 (TLR7/8) Cascade	0.0350	85
Adherens junctions interactions	0.0345	29
Toll Like Receptor 9 (TLR9) Cascade	0.0342	89
Interferon Signaling	0.0333	181
Nucleotide Excision Repair	0.0332	49
BMAL1:CLOCK NPAS2 activates circadian gene expression	0.0324	39
EPHA-mediated growth cone collapse	0.0321	34
Cellular responses to stress	0.0317	278
Signaling by BMP	0.0316	23
Mitochondrial biogenesis	0.0315	47
Influenza Infection	0.0314	122
MyD88:Mal cascade initiated on plasma membrane	0.0313	92
Toll Like Receptor 2 (TLR2) Cascade	0.0313	92
Toll Like Receptor TLR1:TLR2 Cascade	0.0313	92
Toll Like Receptor TLR6:TLR2 Cascade	0.0313	92
Asparagine N-linked glycosylation	0.0310	113
Diseases associated with glycosaminoglycan metabolism	0.0308	26
Diseases of glycosylation	0.0308	26
VEGFR2 mediated cell proliferation	0.0303	33
Cytokine Signaling in Immune system	0.0302	294
Signaling by VEGF	0.0301	112
Post-translational protein modification	0.0301	335
Downregulation of TGF-beta receptor signaling	0.0300	25
Organelle biogenesis and maintenance	0.0296	310

Table 2. Differential pathways for PTC based on DAVID

Pathways	*Count*	*p value*	*Genes*
Integrin cell surface interactions	7	0.0041	*ICAM1, TNC, ITGA2, COL1A1, THBS1, SPP1, FN1*
Hemostasis	12	0.0043	*TFPI, ITGA2, SERPINA1, COL1A1, TREM1, THBS1, MMRN1, ITPR1, PLAU, TGFB1, PLAUR, FN1*
Axon guidance	5	0.0136	*RPS6KA5, NCAM1, COL9A3, ST8SIA4, COL1A1*
Signaling by PDGF	5	0.0329	*COL9A3, COL1A1, THBS1, STAT1, SPP1*
Hormone biosynthesis	4	0.0761	*DIO2, TPO, ALOX5, DIO1*
Metabolism of lipids and lipoproteins	5	0.3224	*LPL, APOE, ABCC3, FABP4, ACACB*
Signaling by Rho GTPases	4	0.4204	*NGEF, TIAM1, ARHGAP36, ARHGAP24*
Signaling in Immune system	6	0.6503	*ICAM1, CFB, ULBP2, COL1A1, TREM1, FN1*
Apoptosis	3	0.7148	*BID, FAS, PMAIP1*
Signalling by NGF	3	0.8591	*RPS6KA5, DUSP4, ITPR1*
Diabetes pathways	4	0.9199	*PCSK2, GNA14, PFKFB2, ITPR1*
Signaling by GPCR	8	0.9707	*GNA14, AGTR1, EDN3, CCL21, CXCL2, AVPR1A, GABBR2, ADORA1*

ing protein, participates in a diverse array of cellular processes, including survival, proliferation and glucose metabolism, and regarded as the unindicted cancer co-conspirator [27]. It could be activated through phosphorylation by a number of kinases, including AKT, protein kinase A, and calcium/calmodulin-dependent kinases and regulated genes whose deregulated expression promotes oncogenesis [28]. Seo et al. found CREB phosphorylation in non-small cell lung cancer (NSCLC) cell lines and pathologic samples from the tumor compared to normal adjacent epithelium [29]. Be-

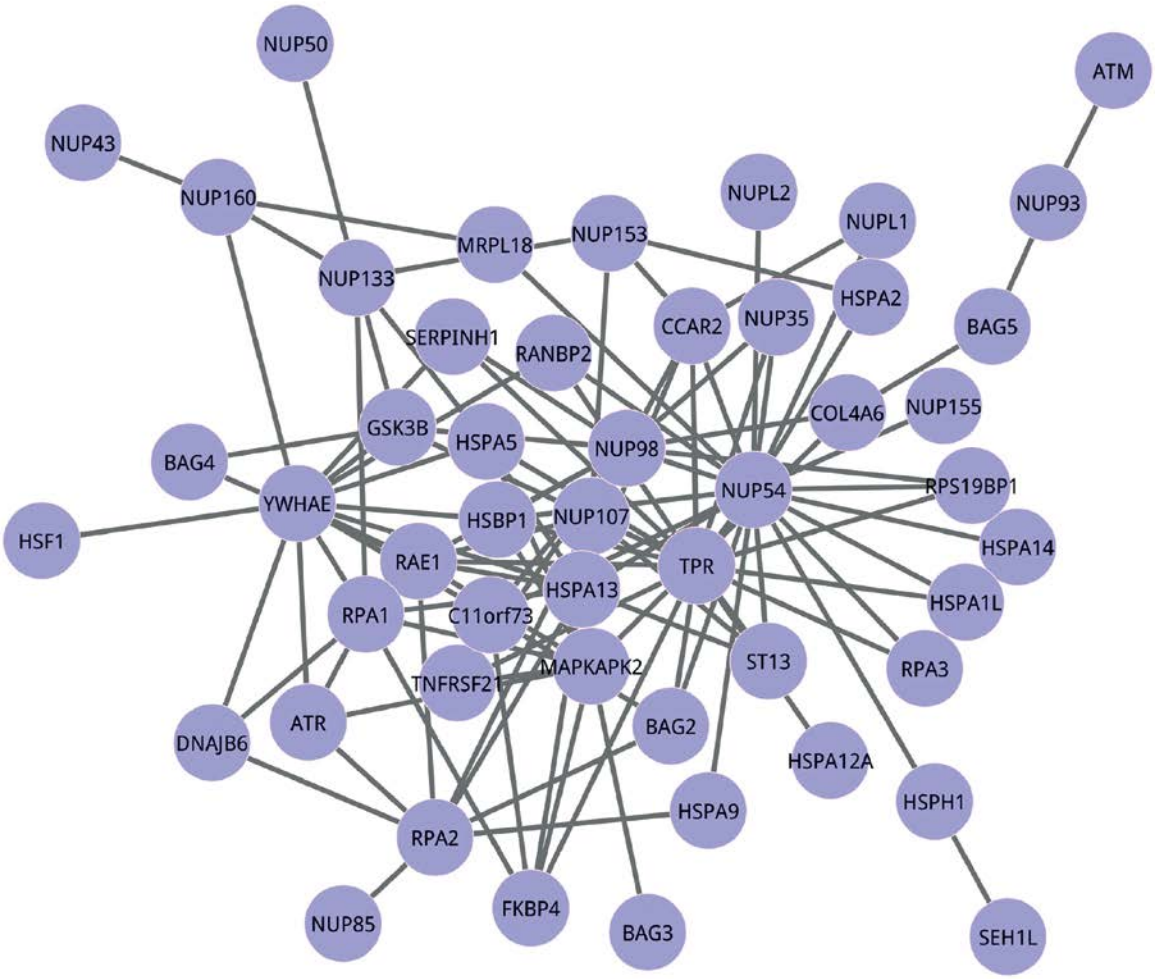

Figure 3. Co-expression network of genes in differential pathway (regulation of HSF1-mediated heat shock response). Nodes are pathway genes, and edges stay for the interactions among genes.

sides, an increased level of phosphorylated CREB was observed in acute myelocytic leukemia, indicating that the protein was functionally active [30]. However, there is no study reporting CREB phosphorylation in PTC, thus this is the first time to reveal the correlation between CREB phosphorylation and PTC.

Attachment of GPI anchor to uPAR and post-translational modification: synthesis of GPI-anchored proteins was also a significant differential pathway between PTC and normal controls. uPAR is a glucose-6-phosphate isomerase (GPI) anchored cell surface protein that is closely associated with invasion, migration, and metastasis of cancer cells [31]. Elevated uPAR expression had been detected in many human cancers, including solid tumors, leukemias and lymphomas [32], and especially the uPAR levels were significantly higher in PTC [33]. Signaling through uPAR activates the tyrosine kinases focal adhesion kinase (FAK) and the MAPK pathway [34] which is a known biomarker in PTC. Therefore, attachment of GPI anchor to uPAR and post-translational modification: synthesis of GPI-anchored proteins were related to PTC closely. In the frame of oncogenesis and cancer progression, glycosylation is the most common post-translational modification of plasma membrane proteins [35].

In conclusion, we successfully identified differential pathways (such as CREB phosphorylation, attachment of GPI anchor to uPAR and post-translational modification: synthesis of GPI-anchored proteins) for PTC using the proposed pathway co-expression method, and these pathways might be potential biomarkers for detection and target therapy of PTC.

Acknowledgements

This research received no specific grants from any funding agency in public, commercial, or not-for-profit sectors.

Conflict of interests

The authors declare no confict of interests.

References

1. Caron NR, Clark OH. Papillary thyroid cancer. Current treatment options in Oncology 2006;7:309-319.
2. Cooper DS, Doherty GM, Haugen BR et al. Revised American Thyroid Association management guidelines for patients with thyroid nodules and differentiated thyroid cancer: the American Thyroid Association (ATA) guidelines task force on thyroid nodules and differentiated thyroid cancer. Thyroid 2009;19:1167-1214.
3. Altekruse S, Kesary C, Krapcho M et al. Cancer Facts and Figures-2010. Institute NC (Ed), SEER Cancer Statistics Review 1975-2007. Bethesda MD: Natl Cancer Inst 2010.
4. Yip L, Kelly L, Shuai Y et al. MicroRNA signature distinguishes the degree of aggressiveness of papillary thyroid carcinoma. Ann Surg Oncol 2011;18:2035-2041.
5. Ellis RJ, Wang Y, Stevenson HS et al. Genome-wide methylation patterns in papillary thyroid cancer are distinct based on histological subtype and tumor genotype. Clin Endocrinol Metabol 2013;99:E329-E337.
6. Network CGAR. Integrated genomic characterization of papillary thyroid carcinoma. Cell 2014;159:676-690.
7. Cohen Y, Xing M, Mambo E et al. BRAF mutation in papillary thyroid carcinoma. J Natl Cancer Inst 2003;95:625-627.
8. Xing M. Molecular pathogenesis and mechanisms of thyroid cancer. Nature Rev Cancer 2013;13:184-199.
9. Glazko GV, Emmert-Streib F. Unite and conquer: univariate and multivariate approaches for finding differentially expressed gene sets. Bioinformatics 2009;25:2348-2354.
10. Dennis G, Sherman B, Hasack D et al. Database for Annotation, Visualization and Integrated Discovery (DAVID). Genome Biol 2003;4:3.
11. Pramana S, Lee W, Pawitan Y. GUI// neaGUI: An R package to perform the network enrichment analysis (NEA). R package version 2013. http://rdrr.io/bioc/nea
12. Wu C, Zhu J, Zhang X. Integrating gene expression and protein-protein interaction network to prioritize cancer-associated genes. BMC Bioinformatics 2012;13:182.
13. Doniger S, Salomonis N, Dahlquist K et al. MAPPFinder: using Gene Ontology and GenMAPP to create a global gene-expression profile from microarray data. Genome Biol 2003;4:R7-19.
14. Dawson JA , Kendziorski C. An Empirical Bayesian Approach for Identifying Differential Coexpression in High-Throughput Experiments. Biometrics 2012;68:455-465.
15. Irizarry RA, Bolstad BM, Collin F et al. Summaries of Affymetrix GeneChip probe level data. Nucleic Acids Res 2003;31:e15-e15.
16. Bolstad BM, Irizarry RA, Astrand M et al. A comparison of normalization methods for high density oligonucleotide array data based on variance and bias. Bioinformatics 2003;19:185-193.
17. Bolstad B. affy: Built-in Processing Methods. http://www.bioconductor.org/packages/release/bioc/vignettes/affy/inst/doc/builtinmethods pdf, 2013.
18. Lee J , Kim D-W. Efficient multivariate feature filter using conditional mutual information. Electronics Lett 2012;48:161-162.
19. Allen JD, Wang S, Chen M et al. Probe mapping across multiple microarray platforms. Brief Bioinform 2012:13;547-554.
20. Taminau J. Using the in Silico Merging package . Citseer 2013. http://insilico.ulb.ac.be/insilico-project.
21. Croft D, O'Kelly G, Wu G et al. Reactome: a database of reactions, pathways and biological processes. Nucl Acids Res 2011;30:691-697.
22. Dawson JA, Ye S , Kendziorski C. R/EBcoexpress: an empirical Bayesian framework for discovering differential co-expression. Bioinformatics 2012;28:1939-1940.
23. Fraley C, Raftery AE. Model-based clustering, discriminant analysis, and density estimation. J Am Statist Assoc 2002;97:611-631.
24. Diboun I, Wernisch L, Orengo CA et al. Microarray analysis after RNA amplification can detect pronounced differences in gene expression using limma. BMC genomics 2006;7:252-266.
25. Da Wei Huang BTS, Lempicki RA. Systematic and integrative analysis of large gene lists using DAVID bioinformatics resources. Nat Protocols 2008;4:44-57.
26. Hosack DA, Dennis G Jr, Sherman BT et al. Identifying biological themes within lists of genes with EASE. Genome Biol 2003;4:R70-77.
27. Conkright MD , Montminy M. CREB: the unindicted cancer co-conspirator. Trends Cell Biol 2005;15:457-459.
28. Sakamoto KM , Frank DA. CREB in the pathophysiology of cancer: implications for targeting transcription factors for cancer therapy. Clin Cancer Res 2009;15:2583-2587.
29. Seo H-S, Liu DD, Bekele BN et al. Cyclic AMP response element-binding protein overexpression: a feature associated with negative prognosis in never smokers with non–small cell lung cancer. Cancer Res 2008;68:6065-6073.
30. Shankar DB, Cheng JC, Kinjo K et al. The role of CREB as a proto-oncogene in hematopoiesis and in acute myeloid leukemia. Cancer Cell 2005;7:351-362.
31. Wang JT, Kerr MC, Teasdale RD. Cancer Insights through Macropinocytosis: A Role for Sorting Nexins? Res Biol Cancer 2014;3:1-23.
32. Alpízar W, Nielsen BS, Sierra R et al. Urokinase plasminogen activator receptor is expressed in invasive cells in gastric carcinomas from high and low risk countries. Int J Cancer 2010;126:405-415.
33. Vincenza Carriero M , Patrizia Stoppelli M. The urokinase-type plasminogen activator and the generation of inhibitors of urokinase activity and signaling. Curr Pharmaceutic Design 2011;17:1944-1961.

34. Giannopoulou I, Mylona E, Kapranou A et al. The prognostic value of the topographic distribution of uPAR expression in invasive breast carcinomas. Cancer Lett 2007;246:262-267.

35. Timpe LC, Haste NV, Litsakos-Cheung C et al. Systemic Alteration of Cell Surface and Secreted Glycoprotein Expression in Malignant Breast Cancer Cell Lines. Glycobiology 2013:23:1240-1249.